Correcting for Circumsolar and Near-Horizon Errors in Sky Cover Retrievals from Sky Images

C.N. Long*

Pacific Northwest National Laboratory, Richland, WA 99352, USA

Abstract: Fractional sky cover amounts retrieved from sky imagery are overestimated significantly at times due to occurrences of "whitening" near the sun, and near the horizon for low sun, in the images. This phenomenon occurs due to forward scattering of visible light by aerosols and haze, and the intensity range limitations of the detectors of the cameras used to record the sky images. Our results suggest that when the problem occurs, the magnitude of the overestimate is typically on the order of about 10% to 20% fractional sky cover. To help alleviate this problem, a statistical analysis of the time series of the areas in the image near the sun position and along the horizon centered on the solar azimuth angle has been developed. This statistical analysis requires that images be captured frequently, at least once per minute. For times when the overestimation is detected as occurring, a correction is applied to the retrieved sky cover amounts. When the sky cover amount correction is applied, analysis indicates that the result better matches the actual sky conditions present, as noted by visual inspection of the sky images in question. In addition, frequency-of-occurrence histogram comparisons show that the adjusted results improve the agreement with other methodologies and expectations. Thus, the methodology presented here helps produce more accurate fractional sky cover retrievals.

Keywords: Sky images, sky cover, clouds, cloud fraction.

1. INTRODUCTION

In the cloudless sky, the area near the sun is most often whiter and brighter than the rest of the hemisphere due to the forward scattering by aerosols and haze. Even a slight haze or moderate aerosol loading will make a large angular area of the horizon whiter and brighter when the sun is low on the horizon. The human eye has an amazing ability to handle a range of light intensity spanning orders of magnitude. One of the problems in using digital cameras such as those used in the sky imager included here is the intensity range limitations of the camera detector. It is desirable to have images bright enough to detect thin clouds, yet this can lead to the part of the image near the sun and near the horizon for low sun appearing whiter in the images than they actually are, not because that is the color perceived by the human eye, but because the commercial imaging elements could produce an exaggerated relative signal. But even for high-quality detectors such as those used in the Whole Sky Imager (Johnson SIORef, 1989) [1], these areas of the image are naturally whiter than other parts of the cloudless sky in the image due to the forward scattering. With no a priori knowledge of the aerosol or haze loading that can be used in some way to predict an increased brightness, these pixels are often interpreted as "cloudy" in the sky-imager retrievals when a human observer would label them as "cloudless." This problem has been recognized previously, for instance by Pfister (JAM. 2003) [2], Sabburg (ACP, 2004) [3]; and Long (JTech, 2006) [4] which briefly described the methodology presented here in broad general terms. In this paper the methodology is described in sufficient detail for readers to be able to apply the methodology. Sky cover retrievals from a commercial instrument, and an equivalent prototype, are analyzed to correct for the overestimation caused by this "whitening" problem. An example long-term analysis is presented to illustrate and verify the impact and utility of applying the correction methodology. Several other long-term analysis results of applying the methodology are included in Long [4].

2. DATA

The U.S. Department of Energy's Atmospheric Radiation Measurement (ARM) Program (Stokes, BAMS, 1994) [5] was established in 1990 to improve the representation of radiative calculations in global models, particularly those involving clouds (Ackerman, PhysToday, 2003) [6]. The ARM Program operates field measurement sites at locations in the central United States, the Tropical Western Pacific area, and on the North Slope of Alaska. One primary measurement need in quantifying cloud-radiative interactions is the amount of cloudiness present at any given time. To help address this need, a cooperative effort between the ARM Program and the National Oceanic and Atmospheric Administration, Surface Radiation Research Branch of the Air Resources Laboratory resulted in the development of a prototype hemispheric sky imager (HSI) system (Long, ProcAMS, 1998) [7]. The HSI was developed and refined as a relatively inexpensive proof-of-concept in using commercially available digital cameras mounted looking downward on a curved mirror to capture hemispheric (horizon-to-horizon) color images of the sky during daylight hours. The HSI prototype is still in service today and is located at the Pacific Northwest National Laboratory (PNNL) in Richland, Washington.

*Address correspondence to this author at the Atmospheric Radiation Measurement Program Pacific Northwest National Laboratory P.O. Box 999, MSIN: K9-24 Richland, WA 99352, USA;
E-mail: chuck.long@pnl.gov

1874-2823/10

The HSI development included the methodology for processing the color sky images to infer the fraction of the sky dome containing clouds. Images of the sky dome are processed for a 160° field-of-view, ignoring the 10° near the horizon where even human observers often have difficulty distinguishing between clear and cloudy due to the scattering associated with the long path length through the turbid atmosphere. Early in the processing algorithm development it was recognized that the areas surrounding the sun in the images, especially when the sun was near the horizon, presented particular problems in inferring whether clouds were present or not. This phenomenon primarily occurs under conditions where few or no clouds are present in the sky dome. As such, a circular area around the sun position in the images (hereafter referred to as the "sun circle") and in an area near the horizon centered on the solar azimuth (hereafter referred to as the "horizon area") were defined and a separate clear/cloudy pixel accounting was included in the processing in addition to the total image accounting. The sizes of the sun circle and horizon areas are set by the user depending on the particular characteristics of the camera being used and the local climatology. For example, if the locality typically exhibits hazy conditions, then these areas would be set larger than for a dry climate which exhibits fewer errors in these areas. For times when there is an overlap between the sun circle and horizon areas, precedence is given to the sun circle, i.e., pixels in the overlapping area are added to the sun circle accounting and not the horizon area. A methodology was then investigated using statistical analyses of the time series of sky cover retrievals to determine whether the pixels labeled as cloudy in these problem areas should be counted as cloudy or not.

The HSI concept was developed subsequently into a commercial instrument called the Total Sky Imager (TSI) model 440 in a cooperative effort with Yankee Environmental Systems, Inc. (YES) under a Small Business Innovative Research grant from the U.S. Department of Agriculture. The image processing methodology was incorporated into the YES TSI Manager software, which also includes user-configurable settings for the sun circle and horizon area separate pixel accounting (Fig. **1**), though not the follow-on analyses described here. TSIs have been deployed at the ARM sites, with the software configured to log the separate "problem areas" pixel accounting in the output. The data from the ARM TSIs and the HSI are used in this study.

Determining the absolute accuracy of sky cover retrievals is problematic due to the lack of an absolute standard. Traditional human observations of sky cover amounts suffer from subjectivity and thus exhibit disagreement. These human observations have also been traditionally recorded as eighths (oktas) or tenths of the sky dome. This means that an uncertainty of 0.125 or 0.10 respectively, is not unexpected. Where human observations of clouds are subjective, decreasing their precision, observation of clouds by automatic devices such as sky imagers is at least objective and highly reproducible.

The Whole Sky Imager (WSI), developed by the Scripps Institution of Oceanography at the University of California at San Diego, is designed to measure radiance at distinct

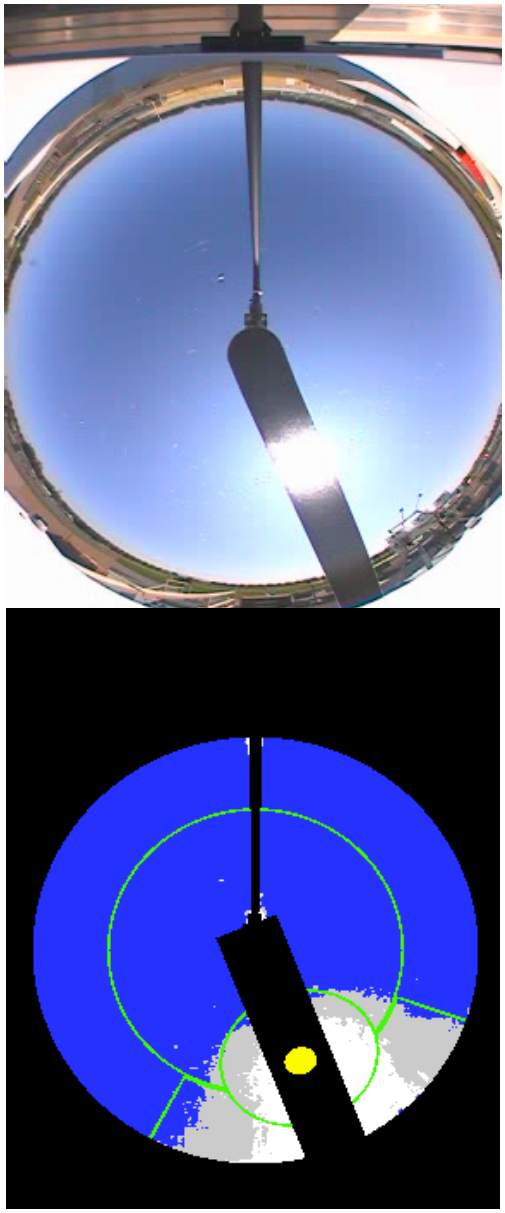

Fig. (1). A sample HSI image (top) and corresponding 160° field-of-view cloud decision image (bottom) taken at 1200 Local time, 20040904 at Pacific Northwest National Laboratory. The dot on the sun-blocking mask in the cloud decision image is the location of the sun in the image, white denotes retrieved opaque cloud, light gray denotes thin cloud, and blue denotes clear sky. The area around the sun outlined in green is the "sun circle" area, the area outlined in green centered on the sun-blocking mask and extending in an arc to either side is the "horizon area." As shown in this example, the two areas contain pixels erroneously determined as "cloud" while the sky image shows clear sky. The large circle centered on zenith is the "zenith circle" used in Section 6.

wavelength bands across the hemisphere [1]. These data can then be used to estimate fractional sky cover, and have been used for this purpose by the ARM Program. A study comparing collocated TSI and WSI sky cover retrievals (Long, ARMTR, 2001) [8] shows that in 87% of the retrievals the absolute difference in total sky cover is less than 5%, and 94% of the time the two retrievals are within 10% total sky cover. Another study comparing TSI sky cover

retrievals with another sky imager in Lauder, New Zealand [2] showed that in about 80% of the retrievals the absolute difference in total sky cover is less than 10%. Thus, although there exists some uncertainty in fractional sky cover retrievals from sky images, this uncertainty does not appear to be greater than that uncertainty attached to human observations for the HSI and TSI retrievals used here.

3. METHODOLOGY OVERVIEW

One characteristic of the sun circle and horizon area cloud misidentification problem is that the erroneously retrieved fractional cloud amount in these areas varies slowly with time. On the other hand, clouds moving across the sky can also move through these areas, causing an increase in variability of the fractional cloud amount over short periods in these areas. Thus, low variability through time can be used as an identifier of when the error might be occurring. Another identifying characteristic is a generally large fractional cloud amount in the problem areas, yet a smaller fractional cloud amount in the remaining parts of the image outside these areas, again with little variability of the cloud amount through time in this remaining area. Finally, it is essentially forward scattering of the direct sun that increases the sky whiteness and brightness causing the problem. Thus the "sun circle" can exhibit circumsolar brightness at all solar elevations, and is a more persistent problem compared to the horizon area where the problem generally only occurs for low sun elevations.

The typical characteristics noted above can be used to test these problem areas and determine whether they should be considered cloudy or not. It must be noted, however, that the sky image sampling needs to be frequent enough for statistical analysis. Kassianov (JAM, 2005) [9] show the typical decorrelation time for sky cover over the entire sky dome to be on the order of about 10-15 minutes. But the sun circle area itself only encompasses a small portion of the sky, meaning that the decorrelation time for the sun circle is also smaller. For these reasons, the time series analysis cannot perform effectively for time series of sky images captured only once every 10, or even 5 minutes. It is recommended that the minimum sampling period be at least once per minute.

4. ALGORITHM OUTLINE

In essence, the magnitude and variability of the cloud fraction in the sun circle, horizon area, and the remainder of the image (total 160^O area minus the sun circle and horizon areas) are used to determine if the cloud pixels in the sun circle and/or horizon area should be included in the total image sky cover estimate or not. In the case of the sun circle, there is also a determination as to whether only some of the original cloud pixels should be counted. The results are smoothed using an 11-point running mean, i.e. if 1 minute data are being processed then the amount of adjustment applied is the average over 11 minutes centered on the point of interest.

We first define a "remainder sky cover" (Rsc) as the sky cover amount remaining after the sun circle and horizon areas are subtracted from the rest of the 160^O processing area. We then define an initial adjustment factor (Sadj) calculated as (1 – Rsc), but limited by a user-configurable amount, typically 0.5. The algorithm calculates a "first guess" for the sun circle by decreasing the amount of the sun circle cloudy pixel count by the initial adjustment factor, i.e. we subtract (Sadj * SCpix) from the total image cloudy pixel amount, where "SCpix" is the number of cloudy pixels in the sun circle. This "first guess" is intended to account for the probability of some error near the sun due to persistent forward scattering for times when the other tests do not subtract the sun circle cloud pixels. There is often some overestimation of cloud amount in the sun circle area, thus the reasoning behind the "first guess" adjustment. This initial adjustment essentially assumes that the cloud amount in the sun circle should be similar to that in the rest of the image after smoothing (discussed later) is applied. Note that this adjustment is to the sun circle cloudy pixels only and is effectively self-limiting. For times when there is not a significant circumsolar problem this adjustment is minimal, making only a small difference to the total sky cover, and only significantly affects the total sky cover for times when the sun circle problem is large, as in the case shown in Fig. (**1**).

For the sun circle/horizon area analyses, we calculate the standard deviation over 21 data samples centered on the time of interest for the sun circle sky cover amount (Sdev), the horizon area sky cover amount (Hdev), and the remainder area sky cover amount (Rdev). We then set user-configurable limits for the acceptable sky cover amounts and variability limits for testing. The exact value of these limits are determined by the performance characteristics of the particular make and model of camera being used.

In the case of the sun circle, we test to see if the sun circle standard deviation (Sdev) is less than the corresponding limit (AdvLim), and the sun circle sky cover amount (Ssc) is greater than the corresponding limit (SscLim). Also, we determine if the sky cover amount in the remainder of the image (Rsc) is less than the corresponding limit (RscLim) and if the remainder area variability (Rdev) is less than the corresponding limit (RdvLim). If all four conditions are met (Sdev<AdvLim, Ssc>SscLim, Rsc<RscLim, and Rdev<RdvLim), then all the sun circle cloud pixels are subtracted from the total cloud pixel amount for the image, i.e., none of the sun circle cloudiness is counted as cloud. If all four conditions are not met, then only the "first guess" sun circle cloud pixels (discussed previously) are subtracted from the total cloud pixel amount for the image.

Similarly, we test to see if the horizon area standard deviation (Hdev) is less than the corresponding limit (AdvLim) and the horizon area sky cover amount (Hsc) is greater than the corresponding limit (HscLim). Also, we determine if the sky cover amount in the remainder of the image (Rsc) is less than the corresponding limit (RscLim) and if the remainder area variability (Rdev) is less than the corresponding limit (RdvLim). If all four conditions are met (Hdev<AdvLim, Hsc>HscLim, Rsc<RscLim, and Rdev<RdvLim), then all of the horizon area cloud pixels are subtracted from the total cloud pixel amount for the image, i.e., the horizon area cloudiness is not counted as cloud.

Once the above determinations as to whether (and how much in the sun circle case) to count the cloudiness or not are made for each individual time sample, then an 11-point

smoothing is applied. The average difference between the original sky cover amount and the adjusted sky cover amount for each time step is calculated over 11 data centered on the time of interest. This running 11-point average amount of adjustment is then applied to the time of interest by subtracting the running average from the original sky cover amount at each time step. This smoothing is applied to more realistically reflect the transitional nature of cloud movement through these problem areas. The determination as to whether to count the cloudiness or not at each time step acts as a step function, but cloud movement into and out of each problem area happens more slowly in time for the highly sampled sky image data. Thus, the smoothing better reflects the way nature acts.

The following is a summary outline of the algorithm described above. First is listed the relevant definition of terms, then Fig. (**2**) shows a flow chart of the algorithm with the horizon area testing path on the left side and sun circle testing path on the right.

DEFINITION OF TERMS

Ssc = Fractional sky cover in sun circle area

Hsc = Fractional sky cover in horizon area

Rsc = Remainder sky cover, all area outside sun circle and horizon areas

Sadj = Sun circle adjustment factor (1 – Rsc)

Sfact = Maximum limit for Sadj

Sdev = Standard deviation of Ssc over 21 data centered on time of interest

Hdev = Standard deviation of Hsc over 21 data centered on time of interest

Rdev = Standard deviation of Rsc over 21 data centered on time of interest

AdvLim = Limit of allowable Hdev and Sdev

RdvLim = Limit of allowable Rdev

SscLim = Minimum limit for Ssc

HscLim = Minimum limit for Hsc

RscLim = Limit of allowable Rsc

SCpix = Total number of cloudy pixels in sun circle

5. EXAMPLE CASE

To illustrate the methodology described above, Fig. (**3**) shows a series of sky images and corresponding cloud decision images for 20040904 at Pacific Northwest National Laboratory, as in Fig. (**1**). The morning was clear, with cloudiness moving in at about 1320 and lasting through about 1520 when skies cleared again. More cloudiness again moved slowly in at around 1700, and slowly moved off through about 1840. As the cloud decision images of Figs. (**1**, **3**) show, this day exhibited significant haze, producing an extreme case of the erroneous identification problem (Fig. **4**), as in Long [4], shows the total sky cover for this daylight period, including the original retrieval, the "first guess" sun circle adjustment, and the final adjusted retrieval using the settings listed in Table **1**.

Fig. (**5**) illustrates the testing involved in the methodology, as outlined in Section 4, for the horizon area testing. Originally, the horizon area cloud amount is retrieved as nearly 100% for most of the morning and afternoon, with some decrease centered on about 1300. All of the horizon area cloudiness is discounted except for the periods from about 1315 through 1510, and 1740 through 1840. For both cloudy periods, Fig. (**5**) shows that the remainder area cloud amount (Rsc) exceeded the set limit (RscLim), thus precluding discounting of the horizon area cloudiness. Additionally, the remainder area standard deviation (Rdev) exceeded the limit (RdvLim) for portions of both cloudy periods, and the horizon area standard deviation (Hdev) exceeded the limit (AdvLim) for portions of the first cloudiness episode. For all other times this day the horizon area cloudiness was not kept as part of the total sky cover amount, resulting in the adjusted horizon area amount shown in Fig. (**5**).

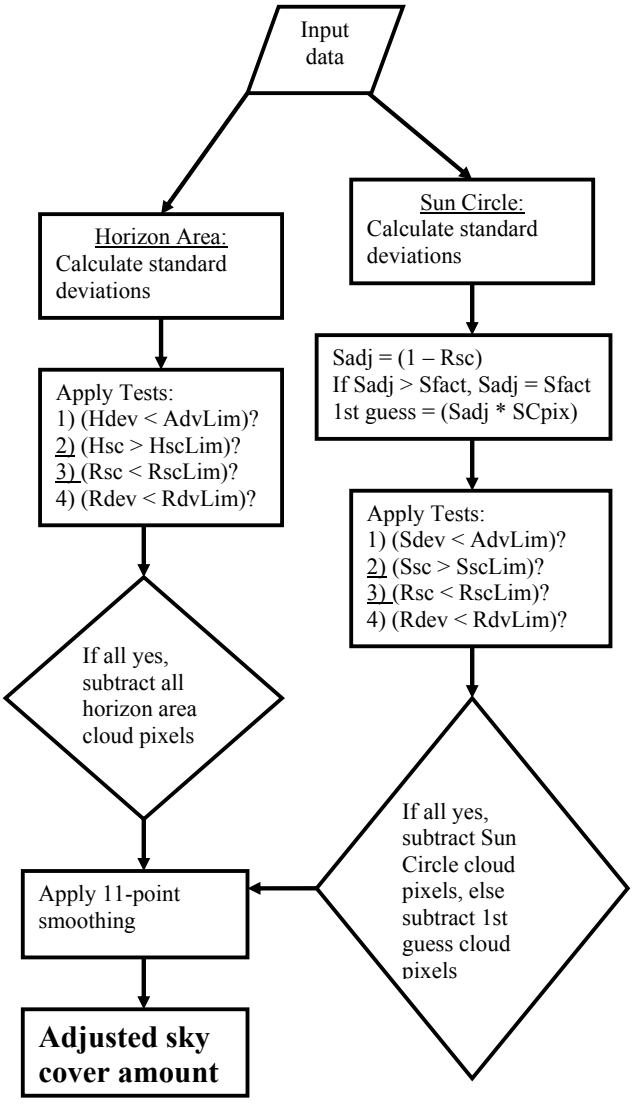

Fig. (2). Flow chart of the algorithm with the horizon area testing path on the left side and sun circle testing path on the right.

Table 1. Limit Settings Used in this Study for Parameters Described in Section 4

Parameter	Setting
Sfact	0.5
AdvLim	0.09
RdvLim	0.05
SscLim	0.3
HscLim	0.2
RscLim	0.2

Similarly, Fig. (**6**) shows the results for the sun circle testing. Originally, the sun circle cloudiness was 100% almost all day, thus at no time on this day did the sun circle standard deviation (Sdev) exceed the corresponding deviation limit (AdvLim). The "first guess" adjustment in general decreases the sun circle cloud amount by about half. For the same periods as noted in Fig. (**5**) for the horizon area, again the remainder area cloud amount (Rsc) exceeded the set limit (RscLim), causing the sun circle cloudiness to revert to the "first guess" amount. Thus the amount of sun circle cloudiness included in the total sky cover is shown by the blue line in Fig. (**6**), where all of the sun circle cloudiness is discounted except for the two previously identified cloudy periods, where about half have been discounted. Note in Figs. (**1**, **3**) that the actual amount of the total sky area for this sun circle, which does not include the sun-blocking strip mask, is minor. Yet, as can be seen in the example sky and cloud decision images, there is often some overestimation of cloud amount in the sun circle area, hence the reasoning behind the "first guess" adjustment.

6. COMPARATIVE ANALYSIS RESULTS

Long [4] presented a comparative analysis of sky cover frequency histograms to verify that the correction methodology presented here in detail improves agreement with other methods of determining sky cover. The analysis included data from more than seven months of data at Pacific Northwest National Laboratory, and for the ARM Cloudiness Inter-comparison Campaign (CIC) field experiment held at the ARM Southern Great Plains site in Oklahoma. The CIC field experiment ran from 20 February through 6 May 2003, providing samples of many variations and types of cloudiness. Fig. (**7**) shows the results for the HSI, similar to the Long [4] Fig. (**7**), along with the difference between the frequency histogram results. The original retrievals show a bias away from the "clear" bin (on the left) toward higher values. This result is at odds with expectations, where it is common that the longer-term frequency distribution for this continental United States mid-latitude site includes about 1/3 clear sky, 1/3 overcast, and the remaining 1/3 distributed in between (Long, ProcAMS, 1999 [10]; Gaustad, ProcARM, 2002 [11]; Long, ProcARM, 2002 [12]). This expected distribution is the case when the adjustments detailed here are applied to the retrievals. In Fig. (**7**) the third distribution (stippled) is from the available 100^{O} field-of-view "zenith circle" retrievals. This zenith area is far less susceptible to the misidentification problems we address, because the entire horizon area is not included and the sun circle problem is generally less for higher sun elevations. There is much better agreement with the adjusted 160^{O} field-of-view distributions (blue difference line in Fig.

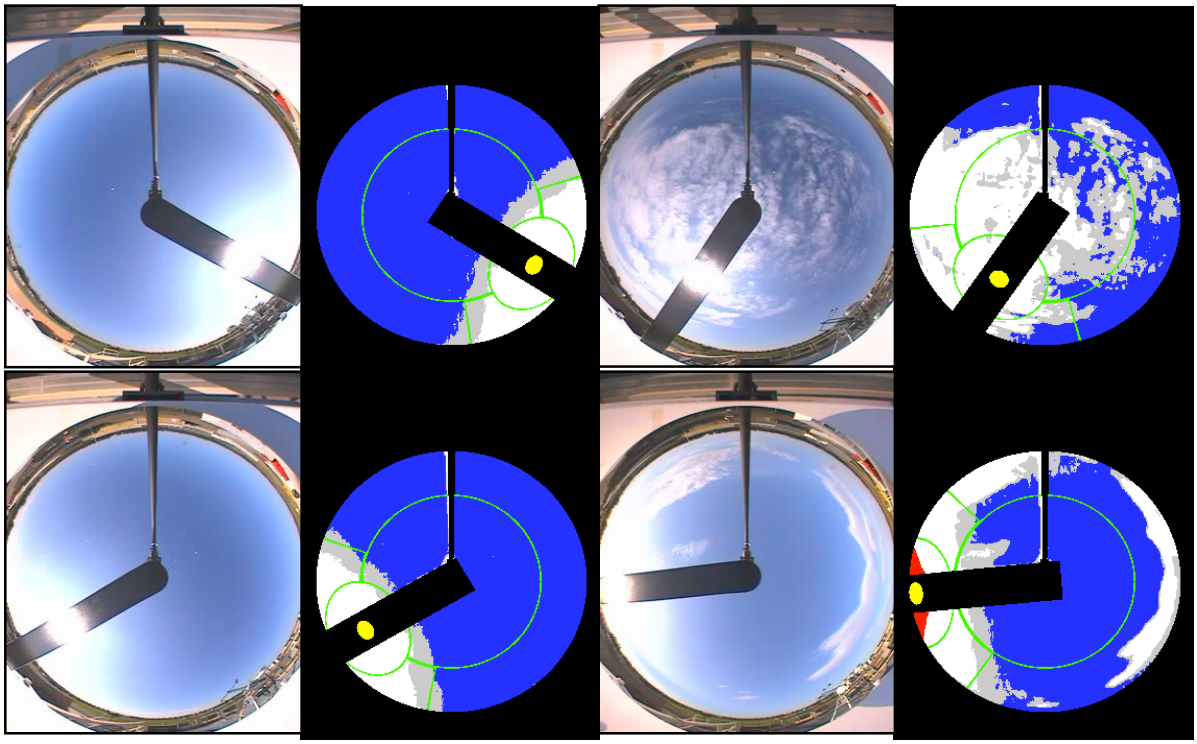

Fig. (3). Same as Fig. (1), but for a series of sky images from 20040904 at Pacific Northwest National Laboratory. Corresponding cloud decision images are to the right of each sky image. Local times of images are 1000 (top left), 1430 (top right), 1600 (bottom left), and 1800 (bottom right).

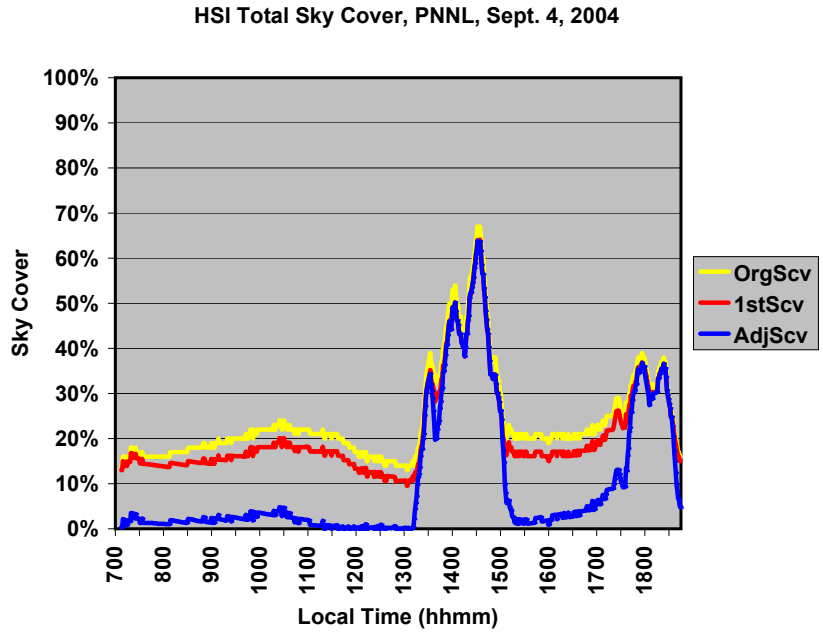

Fig. (4). Total sky cover retrieval for 20040904 at Pacific Northwest National Laboratory corresponding to images in Figs. (**1**, **3**). The yellow line is the original retrieval, the red line is the retrieval including the "first guess" adjustment of the sun circle area, and the blue line is the final result including all adjustments and smoothing, as outlined in Section 4.

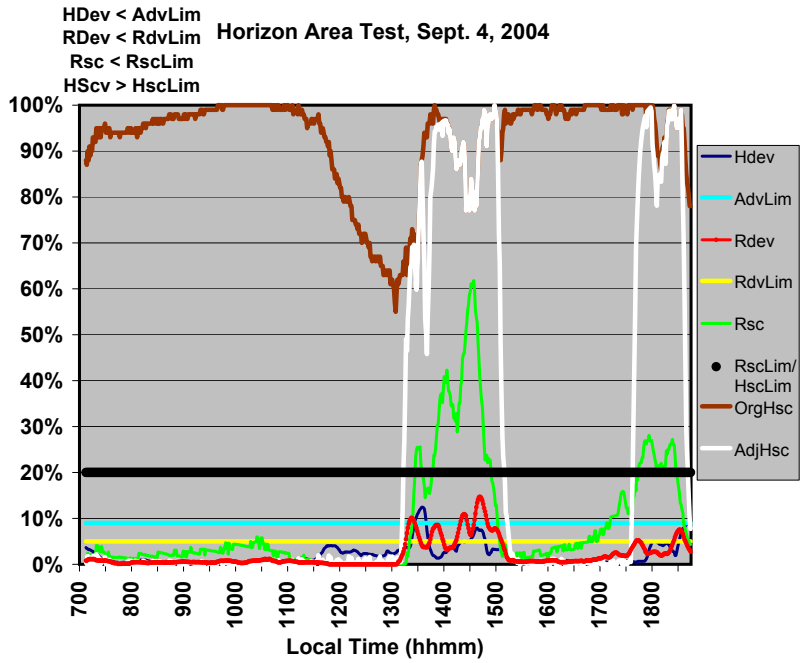

Fig. (5). Horizon area testing results for 20040904 at Pacific Northwest National Laboratory corresponding to Fig. (**4**) adjustments. Brown line is the original horizon area cloud amount, white line is adjusted cloud amount, green is remainder area cloud amount, black line is remainder and horizon area cloud amount limit, red line is the remainder area standard deviation, yellow line is the corresponding remainder area deviation limit, blue line is the horizon area standard deviation, and light blue line is the corresponding horizon area deviation limit.

7) than with the original (red line). Another comparison retrieval in [4] is produced by the Shortwave Flux Analysis [Long, JGR, 2000 [13]; Long, ARM TR, 2004 [14]; Long, JGR, 2006 [15]), a methodology that infers fractional sky cover during daylight periods from an analysis of downwelling shortwave irradiance time series. Long [4] also shows that the Shortwave Flux Analysis results agree better with the adjusted values than with the original unadjusted distribution. All these results suggest that the adjustment methodology significantly improves the sky imager retrievals as intended. Additionally, these results suggest that when the problem occurs, the magnitude of the overestimate is typically on the order of about 10% to 20% fractional sky cover.

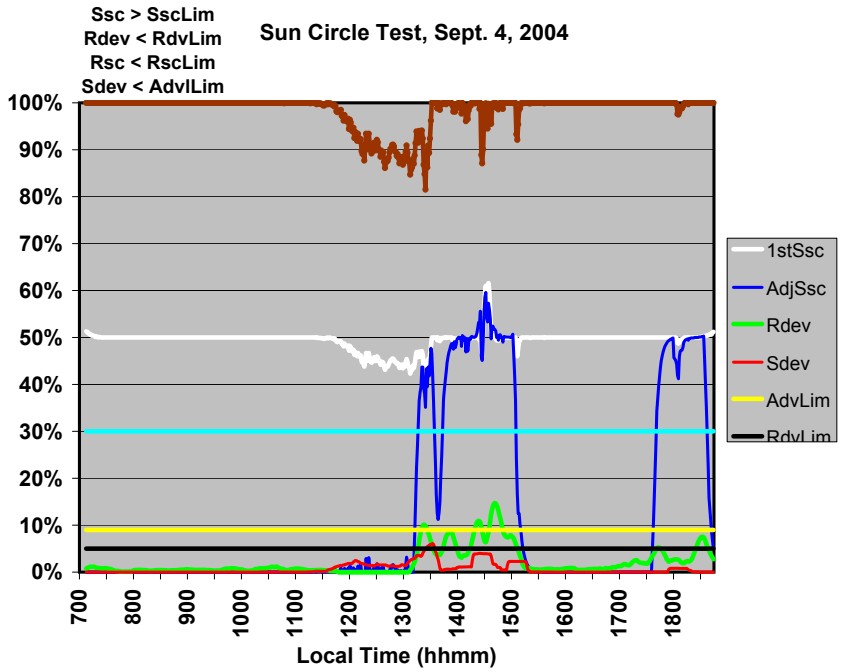

Fig. (6). Sun circle testing results for 20040904 at Pacific Northwest National Laboratory corresponding to Fig. (**3**) adjustments. Brown line is original sun circle cloud amount, white line is the "first guess" adjustment, and blue line is the final adjusted sun circle cloud amount. Red line is the sun circle standard deviation; yellow line is the corresponding sun circle deviation limit, green line is the remainder area standard deviation, black line is the corresponding remainder area deviation limit.

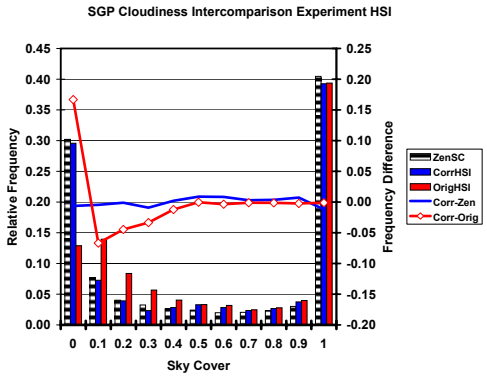

Fig. (7). Sky cover frequency histogram for the HSI deployed during the 3 months of the ARM Cloudiness Inter-Comparison (CIC) field experiment at the Southern Great Plains site. Red columns represent the original uncorrected retrievals, blue the adjusted retrievals, striped represents retrievals restricted to a 100^{O} field-of-view. Blue line (referenced to right axis) is the difference between the adjusted retrievals and the 100^{O} FOV, red line the difference between the original and adjusted 160^{O} retrievals.

The results presented in Fig. (**7**) also suggest that, for long-term statistics of sky cover, a 100^{O} FOV is sufficient. This result is good news for situations where there are significant obstructions in the FOV of the sky imager, as is often the case with the superstructure for ship board deployments. However, this result is true based on the assumption that the narrower FOV experiences the same cloudiness as the larger FOV over sufficiently long time periods, and there is no persistent cloud phenomenon present. For instance Seagal (JAM, 1992) [16] documents the effects of persistent orographically driven convection on global irradiance measurements, which have a hemispheric FOV as sky imagers do. And the early HSI development originally included field testing at the NOAA Surface Radiation Research Branch's Table Mountain site near Boulder, Colorado. Szoke (MWR, 1984) [17] documents a phenomenon known as the Denver Convergence and Vorticity Zone which persistently produces convection during the May to August convection season over the plains to the east of the site, which occurs outside the 100^{O} FOV of a sky imager located there. Thus in these cases, the long term statistics of the 100^{O} FOV, which does not include this persistent cloud phenomenon, would not match the long term statistics of the 160^{O} FOV retrievals. Additionally, we are investigating the retrieval of effective cloud aspect ratio as suggested in Kassianov [9] using two differing FOVs and meeting with significant success. We are using the difference between the 160^{O} corrected and 100^{O} FOV retrievals applied to Equation 9 of [9], and are in the process of verifying the cloud aspect retrievals using time series of cloud radar data. Thus the 100^{O} FOV analysis results here do not suggest that 160^{O} FOV retrievals are unnecessary, as they are certainly of benefit for shorter term analyses and the retrieval of cloud aspect ratio at least.

7. SUMMARY

Whereas human observations of clouds are subjective, decreasing their precision, observation of clouds by automatic devices such as sky imagers is at least objective and highly reproducible. Although there exists some uncertainty in fractional sky cover retrievals from sky images, this uncertainty does not appear to be greater than that attached to human observations for the retrievals used in this study. However, fractional sky cover amounts retrieved from sky imagery are at times significantly overestimated

due to occurrences of "whitening" near the sun and horizon for low sun in the images. This phenomenon occurs due to forward scattering of visible light by aerosols and haze, and the intensity range limitations of the detectors of the cameras used to record the sky images. To help alleviate this problem, a statistical analysis of the time series of the areas in the image near the sun position and along the horizon centered on the solar azimuth angle has been developed. The statistical analysis requires that images be captured frequently, at least once per minute. For times when the overestimation is detected as occurring, a correction is applied to the retrieved sky cover amounts.

When the sky cover amount correction is applied, analysis indicates that the results better match the actual sky conditions present, as noted by visual inspection of the sky images in question. In addition, frequency-of-occurrence histogram comparisons show that the overestimate of sky cover when it occurs is typically on the order of 10% to 20% in sky cover amount, but that the adjusted results improve the agreement with other methodologies and expectations. Thus, the methodology presented here helps produce more accurate fractional sky cover retrievals.

ACKNOWLEDGEMENT

The author acknowledges the support of the Climate Change Research Division of the U.S. Department of Energy as part of the ARM Program. Recognition is also extended to those responsible for the operation and maintenance of the instruments that produced the long-term data used in this study; their diligent and dedicated efforts are often underappreciated.

REFERENCES

[1] Johnson RW, Hering WS, Shields JE. Automated visibility and cloud cover measurements with a solid-state imaging system. SIO Reference 89-7, GL-TR-89-0061, Marine Physical Laboratory, Scripps Institution of Oceanography. San Diego: University of California 1989; p.118

[2] Pfister G, McKenzie RL, Liley JB, Thomas A, Forgan BW, Long CN. Cloud coverage based on all-sky imaging and its impact on surface solar irradiances. JAMA 2003; 42: 1421-34.

[3] Sabburg JM, Long CN. Improved sky imaging for studies of enhanced UV irradiances. Atmos Chem Phys 2004; 4: 2543-52.

[4] Long CN, Sabburg JM, Calbo J, Pages D. Retrieving cloud characteristics from ground-based daytime color all-sky images. J Tech 2006; 23(5): 633-52.

[5] Stokes GM, Schwartz SE. The atmospheric radiation measurement (ARM) program: programmatic background and design of the cloud and radiation testbed. Bull Am Meteor Soc 1994 ; 75: 1201-21.

[6] AckermanTP, Stokes GM. The atmospheric radiation measurement program. Phys Today 2003; 56: 38-44.

[7] Long CN, DeLuisi JJ. Development of an automated hemispheric sky imager for cloud fraction retrievals. In: Proceedings of the 10th Symposium. On Meteorological observations and instrumentation, January 11-16, 1998, Phoenix Arizona Am Meteor Soc 1998; pp. 171-4.

[8] Long CN, Slater DW, Tooman T. Total sky imager (TSI) model 880 status and testing results. Atmospheric Radiation Measurement Program Technical Report, ARM TR-004 2001, Available *via* http://www.arm.gov

[9] Kassianov E, Long CN, Ovtchinnikov M. Cloud sky cover versus cloud fraction: whole-sky simulations and observations. JAMA 2005; 44: 86-98.

[10] Long CN, AckermanTP, DeLuisi JJ, Augustine J. Estimation of fractional sky cover from broadband SW Radiometer Measurements, Proc. 10th Conf. on Atmos. Rad, June 28-July 2, 1999, Madison, Wisconsin.

[11] Gaustad KL, Long CN. An evaluation of cloud cover, cloud effect, and surface radiation budgets at the SGP and TWP ARM sites. In: Proceedings of the 12th ARM Science Team Meeting, St. Petersburg, Florida, April 8-12, 2002.

[12] Long CN, Ackerman TP, Christy JE. Variability across the ARM SGP area by temporal and spatial scale, In: Proceedings of the Twelfth ARM Science Team Meeting Proceedings, St. Petersburg, Florida, April 8-12, 2002.

[13] Long CN. Ackerman TP. Identification of clear skies from broadband pyranometer measurements and calculation of downwelling shortwave cloud effects. JGR 2000; 105(D12): 15609-26.

[14] Long CN, Gaustad KL (2001, Rev. 2004), The shortwave (SW) clear-sky detection and fitting algorithm: algorithm operational details and explanations, Atmospheric Radiation Measurement Program Technical Report, ARM TR-004, Available *via* http://www.arm.gov

[15] Long CN, Ackerman TP, Gaustad KL, Cole JNS. Estimation of fractional sky cover from broadband shortwave radiometer measurements, JGR 2006, 111, D11204, doi:10.1029/ 2005 JD006475.

[16] Seagal M, Davis J. The impact of deep cumulus reflection on the ground-level global irradiance. J Appl Meteor 1992; 31: 217-22.

[17] Szoke EJ, Weisman ML, Browm JM, Caracena F, Schlatter TW. A subsynoptic analysis of the Denver Tornadoes of 3 June 1981. MWR1984; 112: 790-808.

Received: November 4, 2009 Revised: January 30, 2010 Accepted: January 30, 2010